

HENRY

Hydraulic Engineering Repository

Ein Service der Bundesanstalt für Wasserbau

Conference Paper, Published Version

Bey, Alex; Faruque, M. A. A.; Balachandar, Ram; Budkowska, B. B. Role of fluid structures in a two-dimensional scour holes

Verfügbar unter/Available at: <https://hdl.handle.net/20.500.11970/99999>

Vorgeschlagene Zitierweise/Suggested citation:

Bey, Alex; Faruque, M. A. A.; Balachandar, Ram; Budkowska, B. B. (2006): Role of fluid structures in a two-dimensional scour holes. In: Verheij, H.J.; Hoffmans, Gijs J. (Hg.): Proceedings 3rd International Conference on Scour and Erosion (ICSE-3). November 1-3, 2006, Amsterdam, The Netherlands. Gouda (NL): CURNET. S. 73-81.

Standardnutzungsbedingungen/Terms of Use:

Die Dokumente in HENRY stehen unter der Creative Commons Lizenz CC BY 4.0, sofern keine abweichenden Nutzungsbedingungen getroffen wurden. Damit ist sowohl die kommerzielle Nutzung als auch das Teilen, die Weiterbearbeitung und Speicherung erlaubt. Das Verwenden und das Bearbeiten stehen unter der Bedingung der Namensnennung. Im Einzelfall kann eine restriktivere Lizenz gelten; dann gelten abweichend von den obigen Nutzungsbedingungen die in der dort genannten Lizenz gewährten Nutzungsrechte.

Documents in HENRY are made available under the Creative Commons License CC BY 4.0, if no other license is applicable. Under CC BY 4.0 commercial use and sharing, remixing, transforming, and building upon the material of the work is permitted. In some cases a different, more restrictive license may apply; if applicable the terms of the restrictive license will be binding.



Role of fluid structures in a two-dimensional scour holes

Alex Bey¹, M.A.A. Faruque¹, Ram Balachandar² and B.B. Budkowska²

¹Research Associate, Department of Civil & Environmental Engineering, University of Windsor, Windsor, Ontario, Canada.

²Professor, Department of Civil & Environmental Engineering, University of Windsor, Windsor, Ontario, Canada.

An experimental program was carried out to understand the role of fluid structures in a scour hole generated by a plane wall jet. A laser Doppler anemometer was used to characterize the velocity field at various locations in the scour hole region. Observations indicate that different types of fluid structures influence scour at different time periods. Based on the present tests, the entire test duration is divided into five time zones. Following vigorous scour caused principally by jet shear forces and impingement at the start of the test and during early time periods, the flow was characterized by the presence of longitudinal axial vortices, turbulent bursts and movement of the jet impingement point during the later stages. Attempts were made to distinguish the fluid structures at asymptotic conditions. The scour hole region was characterized by the presence of randomly forming and disappearing streaks, laterally located concave shaped depressions, rolling and ejection of the bed material. Through analysis of higher order moments, sweep and ejection type events were observed, which can potentially contribute to scour.

I. INTRODUCTION

Laboratory studies of the interaction of plane wall jets with non-cohesive sand beds and other forms of two-dimensional jet scour have been carried out to understand the mechanisms of scour. As rightly pointed out by Ref. [5], a comprehensive understanding of the scour mechanisms remains elusive because of the complex nature of the flow field. The hydrodynamic characteristics of the jet flow, and the concave shape of the eroded bed further increases the complexity. The physical properties of the sediment as well as the turbulent flow field characteristics are equally responsible for the entrainment, suspension, transportation and deposition of the sediment. Details of several other previous studies involving two-dimensional jet scour are available in Ref. [3] and avoided here for brevity. Recently, Ref. [1] noted the need to understand the role of turbulent fluctuations in scour analysis.

In a recent study, Ref. [6] suggest that sediment transport, and the resulting scouring mechanism was due to turbulence created by Görtler vortices as a result of the destabilization of the turbulent wall layer by the concave curvature of the water sediment interface. They also proposed new scaling laws relating time and the attainment of the quasi-steady scour depth.

Concurrent with the development and evaluation of mathematical models, it is necessary to understand the flow features that influence the scour process. The present study was carried out to obtain the velocity field

in the scoured region and to further understand the role of turbulent flow structures that influence scour. To this end, velocity measurements were conducted within the scour region at asymptotic conditions. Besides the mean flow, the higher order velocity moments were evaluated to understand the role of turbulent events.

II. EXPERIMENTAL SETUP AND PROCEDURE

The experiments were performed in a recirculating open channel flume which is 15 m long, 0.4 m wide and 0.9 m deep. The nozzle width is 0.4 m wide with an opening $b_o = 25$ mm, and is set flush with a horizontal non-cohesive bed (0.3 m deep, 0.4 m wide and 2.5 m long). The median grain diameter, d_{50} is 2.15 mm with a geometric standard deviation σ_g of 1.28. The bed material can be classified as very fine gravel. The bed was fully saturated prior to the start of the tests. The flow conditions were maintained to obtain local scour and there was no net transport of material beyond the edge of the bed.

Two tests were conducted uninterrupted at a tailwater depth (H_t), corresponding to $20b_o$. The present tests can be classified to be under the high submergence flow regime. The jet exit velocity (U_o) for the two tests (denoted as A and B) was held constant at 1.0 m/s and 1.27 m/s, respectively. These correspond to jet exit Reynolds numbers ($Re_j = U_o b_o / \nu$) of 25,000 and 32,000 respectively. The densimetric Froude numbers $F_o = U_o / \sqrt{g(\Delta\rho/\rho)d_{50}}$ are 5.4 and 6.8, respectively. It should be remarked that the test at $U_o = 1.0$ m/s (Test A) was repeated thrice, mainly to ensure repeatability and also to obtain confirmation of flow features that were noticed. The scour profiles were obtained using a digital point gauge having a resolution of ± 0.01 mm.

The test duration extended over a period of 8-12 days even though an asymptotic state of scour was noted to be attained earlier on. Based on the rate of growth of the scour hole and mound, one can define an asymptotic condition as a state beyond which no significant changes in geometry occur. Sectional and plan view of the scour region along with the definition of variables is shown in Figure 1a. Figure 1b shows the variation of the important scour parameters with time. Depending on the scour hole/mound geometric parameter chosen, the time to achieve an asymptotic state can be as low as $t = 24$ hours. For example, the total length of the scour affected region (L_T) attains an asymptotic state at $t = 24$ hours, while the change in the maximum depth of the

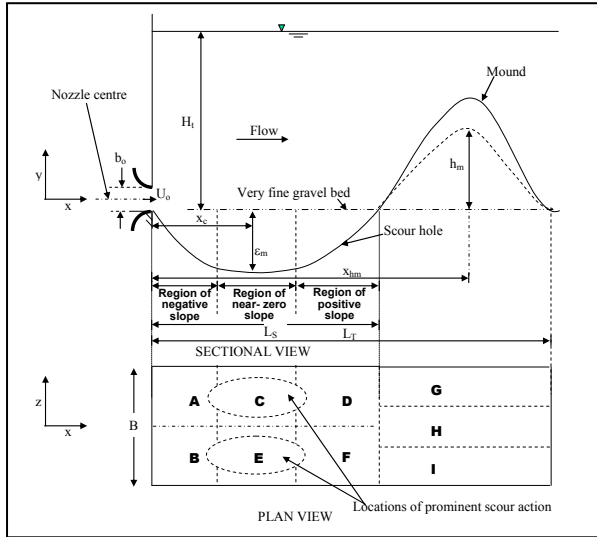


Figure 1a: Definition sketch.

scour hole (ϵ_m) is less than 5 % from $t = 48$ hours and beyond. However, it should be noted that beyond 72 hours, there is the presence of the turbulent bursts which cause local changes in the location of the maximum depth of scour hole (x_c) but no significant changes in the mean scour profile. In this study, the asymptotic condition has been defined as a state when no significant change in any of the scour parameters is noticed. Detailed velocity measurements were conducted well beyond the 72-hour period.

For each test, the uniformity of the velocity distribution across the nozzle exit was verified. Further, constancy in test conditions was ensured by monitoring the velocity at the nozzle exit over the entire test duration (8 ~ 12 days). The velocity measurements were carried out with a non-intrusive two component fiber-optic LDA operated in backward scatter mode. The presence of glass side walls of the flume provided optical access to the laser beams. Details of the LDA system are available elsewhere (Ref. [4]) and not included here for brevity. At asymptotic conditions, velocity profiles were obtained along the flume axis at various axial stations covering a range $2 \leq x/b_0 \leq 50$.

The scour hole shape as a function of time, sediment movement in the scour hole and its variation across the width of the channel was studied with a video imaging system. Dye injection was used to enhance flow visualization. In this study, U and V denote the velocity in the x and y direction respectively, while u and v denote the fluctuations about the mean. The time averaged quantities are denoted by an over bar.

III. RESULTS AND DISCUSSION

Effect of time:

The following observations were made with the aid of dye injection and observing the movement of bed particles at various locations in the flow field. Distinct types of scour phenomena were observed in five different time ranges. These time zones were chosen based on a detailed review of the video tapes and observations made during repeated experiments. A time scale, defined by $T = L_S/U_0$ is defined in the present study and is used to non-dimensionalize the time zones. Here, L_S is the length of

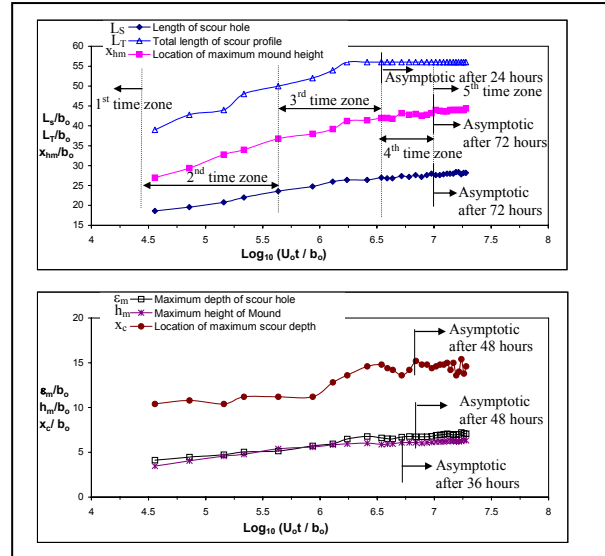


Figure 1b: Variation of scour parameters with time.

the scour hole at asymptotic conditions (Figure 1a). It should be remarked that another parameter such as ϵ_m or x_c could have been chosen to represent length scale. However, on repeated viewing of the tapes, L_S was found to be consistently easier to measure and more sensitive as an indicator of asymptotic state. Figure 1b also depicts the five time zones and one can notice that the rate of change of scour (for example, see change in slope of L_S vs. time or x_{hm} vs. time) more-or-less can be correlated with the time zones. The five time zones are described below:

a) $t/T \leq 850$: When the plane wall jet exits the nozzle, the flow is initially parallel to the bed and following a very short duration, scour commences. Scour is very vigorous and a negative slope region is quickly established (see Figure 1a). A hole is formed downstream of the nozzle and the very fine gravel particles are deposited as a mound further downstream. In this time zone, the scour hole and mound are fairly two dimensional. The size of the hole is gradually increased with the increase in the length of the negative slope region. Due to the jet impingement action, most of the downstream grain movement occurs in the near-zero or positive bed slope region. As the scour hole progresses in the longitudinal direction, the jet impingement on the downstream slope of the hole causes a large scale suspension of bed material into the flow. An example of this suspension at early stages of the scouring process is shown in Figure 2a. Though not shown in the figures, video images indicate that grains are suspended all the way to the free surface ($\sim 20 b_0$). The particles are predominantly transported in the downstream direction though some fall back into the scour hole.

b) $850 \leq t/T \leq 15 \times 10^3$: With progress in time ($t > 600$ s for Test A), the jet expands into a larger space (due to the presence of a larger and deeper scour hole). The jet is confined by the bed on one side and can be considered to be relatively free on the other side. The large scale suspension of the bed material seen earlier is reduced significantly (Figure 2b). In this time zone, the bed particles are carried in the vertical direction up to about $6 \sim 8 b_0$. There is very little scour that occurs in the negative slope region. It has been reported in previous

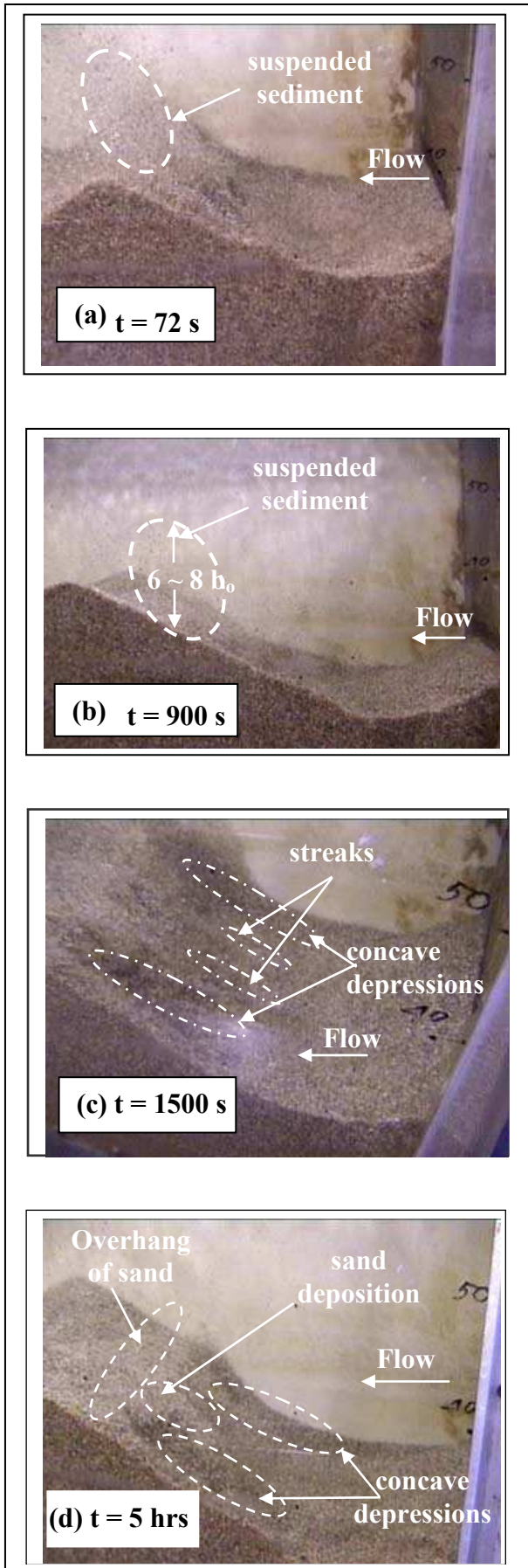


Figure 2: Images illustrating scour process.

studies that the negative slope quickly attains an equilibrium condition while most of the scour occurs downstream. In the negative slope region, the bed material moves towards the nozzle due to the formation of a recirculating flow. The grains also roll down the negative slope but no major scour occurs in this region. Most of the downstream grain movement continues to occur in the near-zero or positive bed slope region. Two well defined concave shaped lateral depressions stretching from region C into region D (and from E to F, Figure 1a) are formed. One can also observe two to three longitudinal streaks, that form and disappear rapidly in the scour hole region accompanied by lateral motion of bed particles. The presence of these streaks cause the very fine gravel to be deposited as small longitudinal ridges. Figure 2c shows the scour hole at $t = 1500$ s with two streaks and two concave depressions. The streaks are very similar to that noticed by Ref. [6]. However, Ref. [6] did not report the presence of the concave shaped depressions. The concave depressions on either side of the streaks are very prominent. The formation and disappearance of the streaks continue for a relatively significant period. Ref. [6] observed loose sediment streaks or longitudinal ridges on the positive bed slope in the scour hole while in the present tests, the streaks were observed mostly in the near-zero bed slope and at the beginning of positive bed slope. They mentioned that streaks or longitudinal ridges represented signature of intense longitudinal vortices which lift up the sediment. They attributed these vortices to Görtler instability and have shown that the flow conditions favour such instability. In the present tests, systematic formation of loose streaks was not observed although there was the tendency for the formation of one or two very unstable short streaks. It is important to point out that Ref.[6] conducted their experiments in the submergence range of 2.75 to 8.8, which is much lower than that used in the present study. As indicated earlier, tests in this range of submergence have been noted to be strongly influenced by flicking of the jet towards the bed and free surface in an alternate manner (Ref. [2]).

c) $15 \times 10^3 \leq t/T \leq 125 \times 10^3$: After about 3 hours when scour had progressed sufficiently, the streak like features became less prominent. On either side of the flume axis, there appeared a 'scoop and throw' like scouring action which caused longitudinal concave shaped depressions and is represented in Figure 2d. This is once again in the region C-D and E-F in Figure 1a. The bed appears to be fluidized at the end of these concave shaped depressions and particles are carried by the flow downstream into the mound region. A portion of the bed particles accumulate on the upstream face of the mound and in between the two concave shaped depressions and eventually slide back into the depressions when their apparent weight is greater than the sweeping force of the fluid. The 'scoop and throw' like action is then momentarily arrested.

One can also observe a lifting spiraling motion of bed particles near the end of concave shaped depression, indicative of some type of vortex activity. Dye visualization in the near bed region confirms vortex like structures and the sudden acceleration of the flow at the end of the scooped region. The presence of the vortices was also confirmed by observing the motion of individual grains.

d) $125 \times 10^3 \leq t/T \leq 375 \times 10^3$: ‘Scoop and throw’ like scouring action slowed down after 24 hours. Progress of scour continues but at a slower pace. Concave shaped depression caused by ‘scoop and throw’ mechanism is not that apparent at this stage but small scale suspension of bed material provides evidence of ‘scoop and throw’ action. One can notice small scale bed suspension on one side of the flume axis in Figure 2e (which shows the near-bed region only). The suspension of a very few grains extends to about $1 \sim 2 b_0$. This subsided ‘scoop and throw’ action continues up to 72 hours. Dye injection confirmed the presence of spiral motions during this time period. Figures 2f to 2h show images of the flow field in the near-bed region at $x/b_0 = 10$. The dye is injected by a ‘L’ shaped tube with the exit port facing the near wall of the flume. In Figure 2f, the dye initially flow towards the near side wall (out of the picture) and spirals towards the upstream direction. In Figure 2g, the dye injection is shown 2 s later than that in Figure 2f. The dye now exits the port and flows towards the far wall. In Figure 2h (which is acquired 4 s later than Figure 2g), the dye flows in the downstream at a slight angle to the streamwise direction. Collectively, using images such as Figure 2f to 2h and several video frames, a clear spiraling motion can be deciphered.

e) $t/T > 375 \times 10^3$: About 72 hours into the scour process, when the scour hole attains an asymptotic state, what can be described as turbulent bursts were noticed to occur in the near-bed region across the cross-section of the flume. Figure 2i and 2j show images with and without turbulent bursts separated by a time interval of 2 s. The effect of the burst can be noticed by the suspension of bed particles. These bursts were frequent and occurred randomly. Furthermore, they caused the movement of bed particles close to the bed region in all directions. The transport in the vertical direction is less than b_0 . This type of activity is visible in a section beyond the maximum scour depth location (x_c in Figure 1a). In addition, at asymptotic conditions, two prominent scour mechanisms were observed to occur on either side of the flume axis and as shown in Figure 2k. As a consequence of these mechanisms, bed particles were laterally moved from the region. Particles appeared to be spiraled towards the side walls and the flume axis. However, no longitudinal particle movement was observed along the nozzle axis. These two scour mechanisms occurred quite frequently and as measured by the movement of bed particles, the two fluid structures causing the scour appear to be identical in strength as the bed contour was symmetrical about the flume axis. Occasionally, one would note that one of the two structures was stronger than the other, and this caused lateral movement towards the weaker side. This momentarily caused the bed contour to become asymmetrical. No preferential occurrence on one or the other side of the flume axis of the stronger structure was noted. It should be remarked that at asymptotic conditions, the back and forth movement of the impingement point (discussed in a later section), the frequent but random turbulent bursts and the two prominent scour mechanisms, all occurred at one time or the other. The jet impingement tends to cause a limited suspension and lifting of the bed particles into the flow stream where they are picked up and transported by the higher velocity fluid parcels. In addition, the fluid structures caused lateral particle movement. It is however

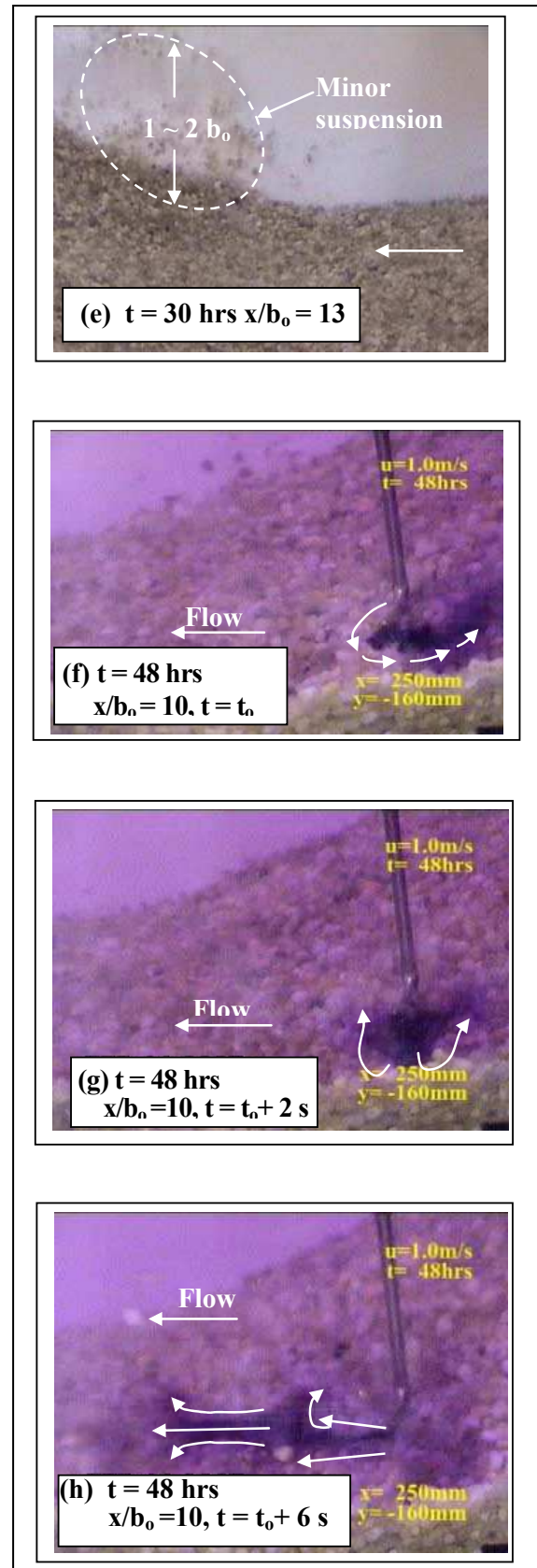


Figure 2 (cont'd): Images illustrating scour process.

note worthy that in spite of these actions, any changes in the instantaneous bed profile was a local phenomenon and did not cause significant change in the overall mean

bed profile. It should also be noted that at the asymptotic state, scour profile in the hole region is nominally two-dimensional across the width of the flume. However, at the mound region, the lateral profile is not two-dimensional and has two distinct peaks (Region G and I of Figure 1a). These peaks occur closer to the side walls leaving a trough in center portion of the mound (Region H of Figure 1a).

Presence of vortex in ‘scoop and throw’ regime:

As indicated in the previous section, two counter rotating vortices were seen to occur in the scour region (for the time period $15 \times 10^3 \leq t/T \leq 375 \times 10^3$). The presences of the vortices were confirmed by dye visualization and movement of fine gravel particles in the scour hole. Figures 3a to 3d shows the vertical component velocity histogram at $x/b_0 = 14$ for Test A. Negative V will indicate downward directed motion. Since the laboratory is equipped only with a two-dimensional LDA system, the third velocity component (W) could not be directly obtained. Additional measurements were made by placing the LDA probe at an angle with the streamwise direction and the arrangement is indicated as an insert in Figure 3e to obtain an estimate of velocity in the z direction. Figures 3e to 3h show the velocity histogram obtained in the plane of measurement indicated in the inset of Figure 3e. Negative value of this histogram indicates motion towards the near side wall and positive value of the same indicates motion towards the far side wall. As indicated in the histograms, the number of negative measurements decreased as one goes up from the near-bed location. These measurements are only qualitative and used to evaluate the fluid motion towards the wall. Together with the vertical velocity measurement (Figures 3a to 3d), one can clearly see a rotational type motion that is directed towards the inner side wall in the bottom regions and away from the inner side wall for the upper locations and serves to confirm the presence of a vortex structure.

Asymptotic conditions:

As indicated earlier, detailed velocity measurements were conducted at an asymptotic state when there was no significant change in the scour conditions. The impingement of the jet on the bed is first discussed followed by the variation of the mean velocity and higher-order moments.

Jet Impingement: During the progress of the scour hole, visual observation indicates that the jet impingement point moves back and forth. This can be confirmed by the presence of upstream and downstream movement of particles near the bed in the range $0 < x/b_0 < 16$. Figure 4 shows the histogram of streamwise velocity along the scoured bed for Test B at various locations ($10 < x/b_0 \leq 20$). These locations extend from the end of the negative bed slope region to the start of the positive bed slope region as indicated in Figure 4b. One can note from the graphs that, for $10 < x/b_0 \leq 13$ (Figures 4a, 4c to 4e), although the streamwise mean velocity is very low near the bed, the instantaneous velocity varies over a wide range from -0.8 m/s to 1.0 m/s. The histograms have two distinct peaks and one can also note that the negative instantaneous velocity constitutes a significant percent of the total realizations, which is a

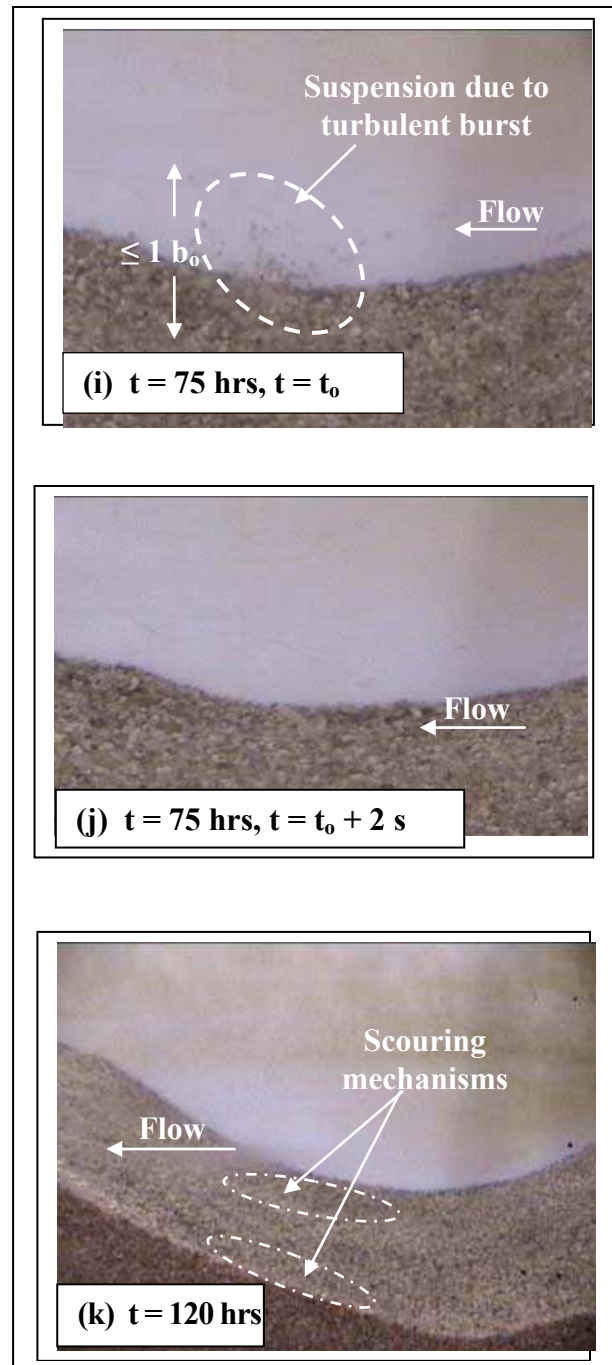


Figure 2 (cont'd): Images illustrating scour process.

clear indication of back and forth movement of jet impingement point. For $x/b_0 \geq 14$ (Figures 4f to 4h), the value of mean streamwise velocity increases and the negative instantaneous velocity count decreases. For the location of $x/b_0 = 20$ (Figure 4i), the negative instantaneous velocity count is less than 10%, and the overall histogram tends to have a single peak with more turbulence like fluctuations rather than back and forth jet movement. This is an indication that the jet impingement point extends up to about $x/b_0 \approx 18$ with a mean location (defined as the location where 50% of velocity realizations are negative) occurring around $x/b_0 \approx 13$.

Mean velocity profiles: Figure 5 shows the velocity vector plots for test A in the scour hole region at

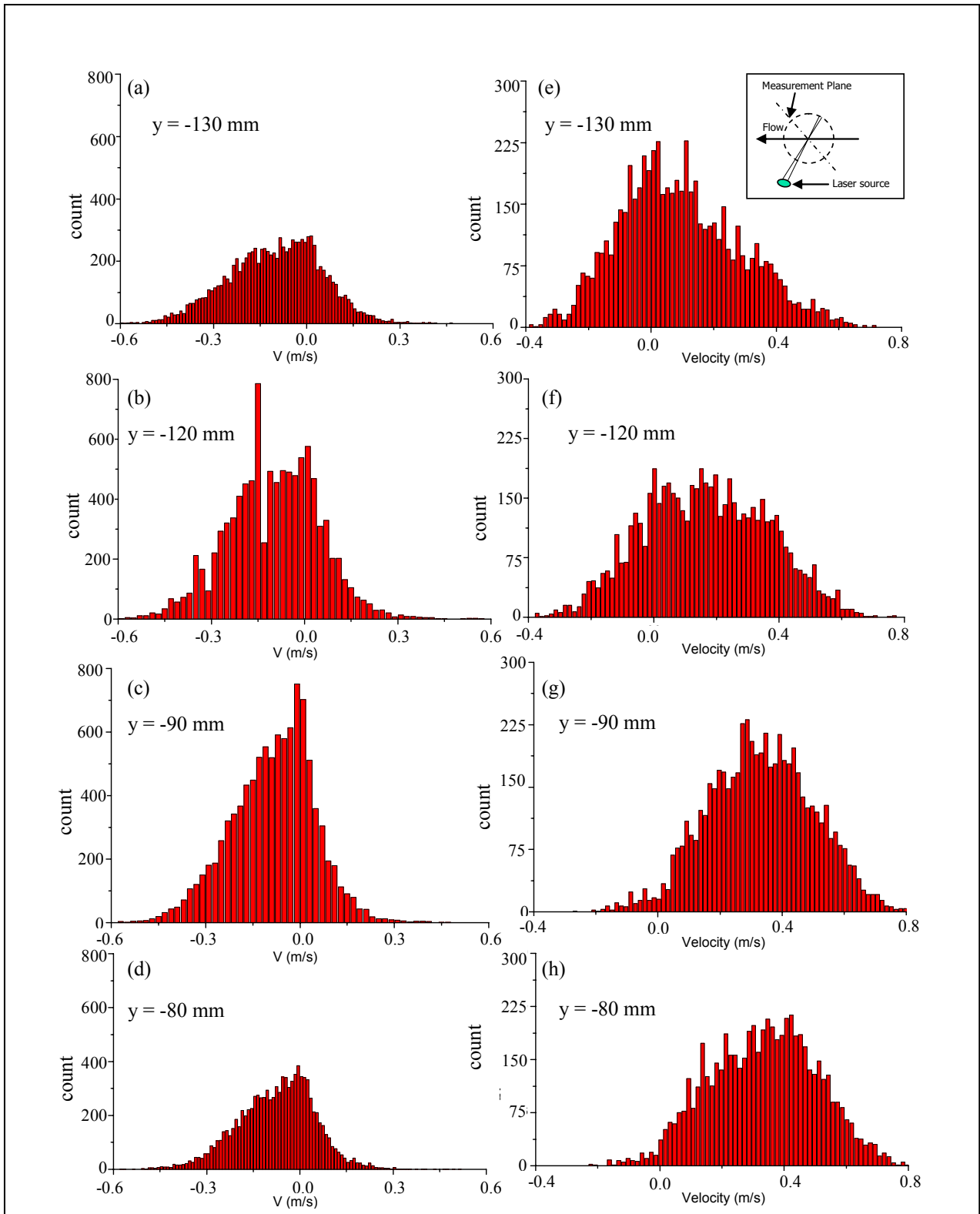


Figure 3: V histogram and estimate of W histogram at $x/b_0 = 14$.

asymptotic conditions. One can clearly see from the vector plots that the jet expands and interacts with the bed. In the region above the jet, there is a large scale recirculating region which extends to about $35b_0$ downstream. The center of this region is located at about $16b_0$ along the x axis and about $10b_0$ along the y axis. It is important to recognize that this recirculation region

provides for a significant downward velocity component near the nozzle. The impingement of the jet also generates a recirculating flow in the bed region close to the nozzle. A similar velocity plot was obtained for Test B which is qualitatively similar to that obtained in Test A. The mean impingement point in Test B occurs farther from the nozzle and consequently has a larger near-bed recirculation zone.

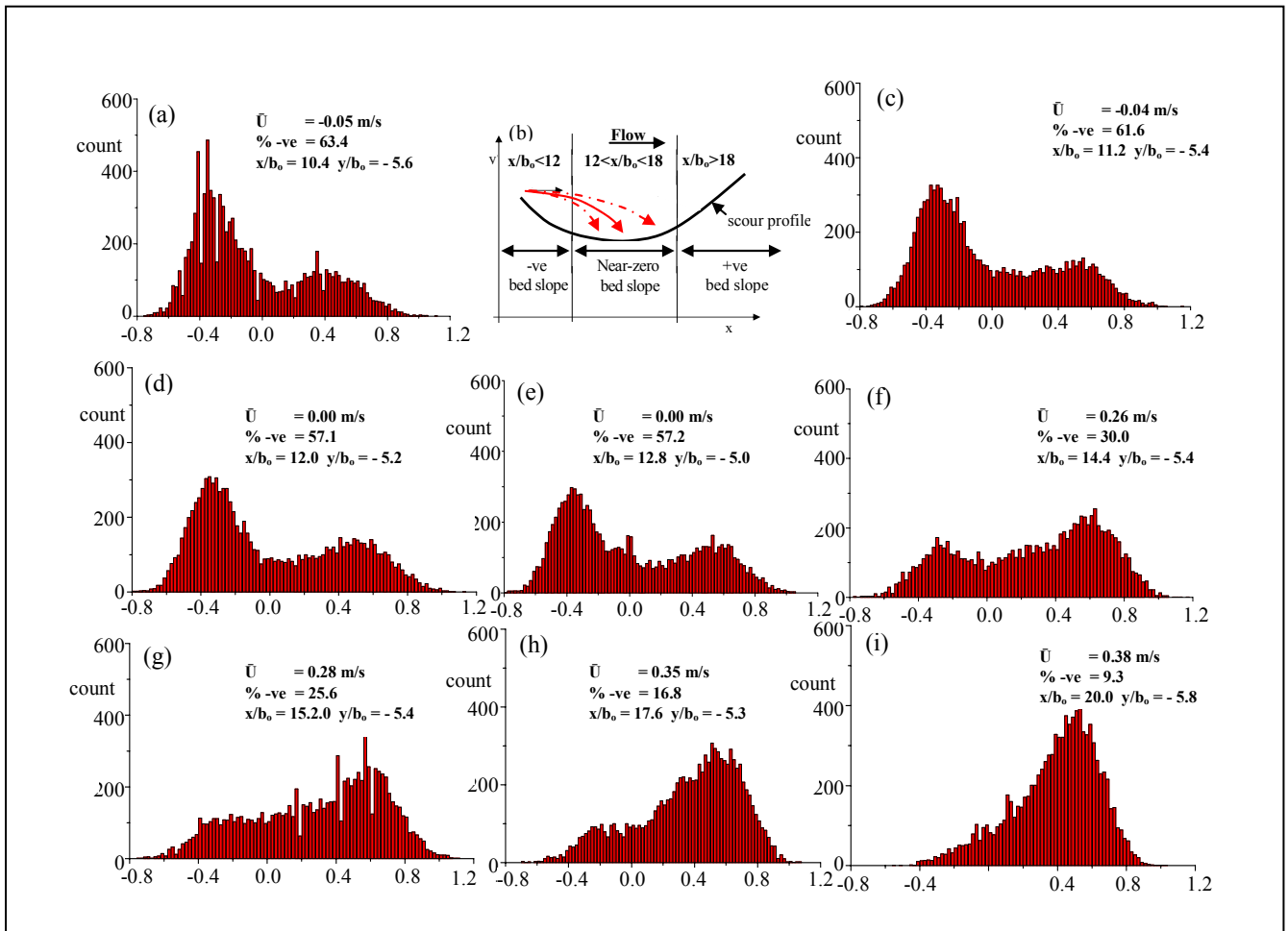


Figure 4: Histogram of streamwise velocity distributions along the scour bed for Test B.

In progressing from near the nozzle to several downstream stations, the jet expands. The locus of the maximum velocity moves downwards away from the nozzle axis which is indicative of the jet bending. Clearly, the jet expands asymmetrically and the computed rate of expansion was found to be higher than free jets. The bottom half of the jet displays a greater half-width than the upper half of the jet. Moreover, it is clear that, the jet begins to bend very early on and is different from a free jet. This is different from the observation of Ref. [7] who noted the jet characteristic to be similar to that of a free jet up to the point of maximum scour.

Higher order moments: Figure 6 shows the variation of turbulent diffusion in the y direction, $D_v = \overline{u^2 v}$ and the variation of $\overline{u^3}$ which can be thought as the streamwise flux of the turbulent kinetic energy $\overline{u^2}$ at various axial stations. The values for $\overline{u^2 v}$ and $\overline{u^3}$ above $y/b_0 = 3$ are close to zero and therefore makes no significant contribution to the discussion on the effect of turbulence on scour. The nine sets of profiles are divided into 3 rows, depending on the location with respect to the maximum scour depth. Figures 6a to 6c are in region of negative bed slope, Figures 6d to 6g are in the region of

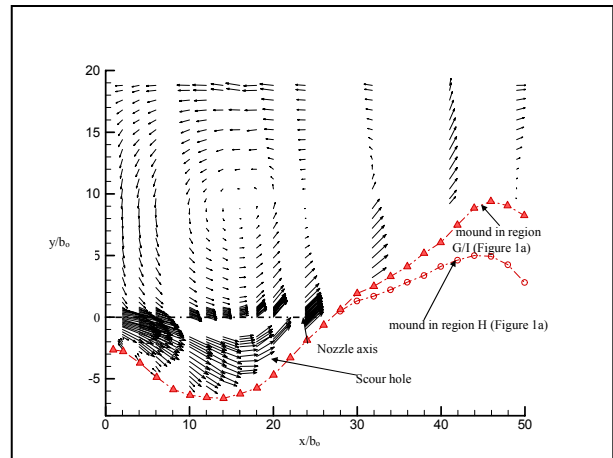


Figure 5: Velocity vector plot for Test A.

near-zero scour slope, while Figures 6h and 6i are in the region of positive bed slope.

Figure 6a shows that both D_v and $\overline{u^3}$ are close to zero near the bed. As one progresses from the bed towards the free surface, absolute values of both D_v and $\overline{u^3}$ increase and attain local peaks at almost the same level ($y/b_0 = -1.6$) but with opposite signs. D_v has a negative peak

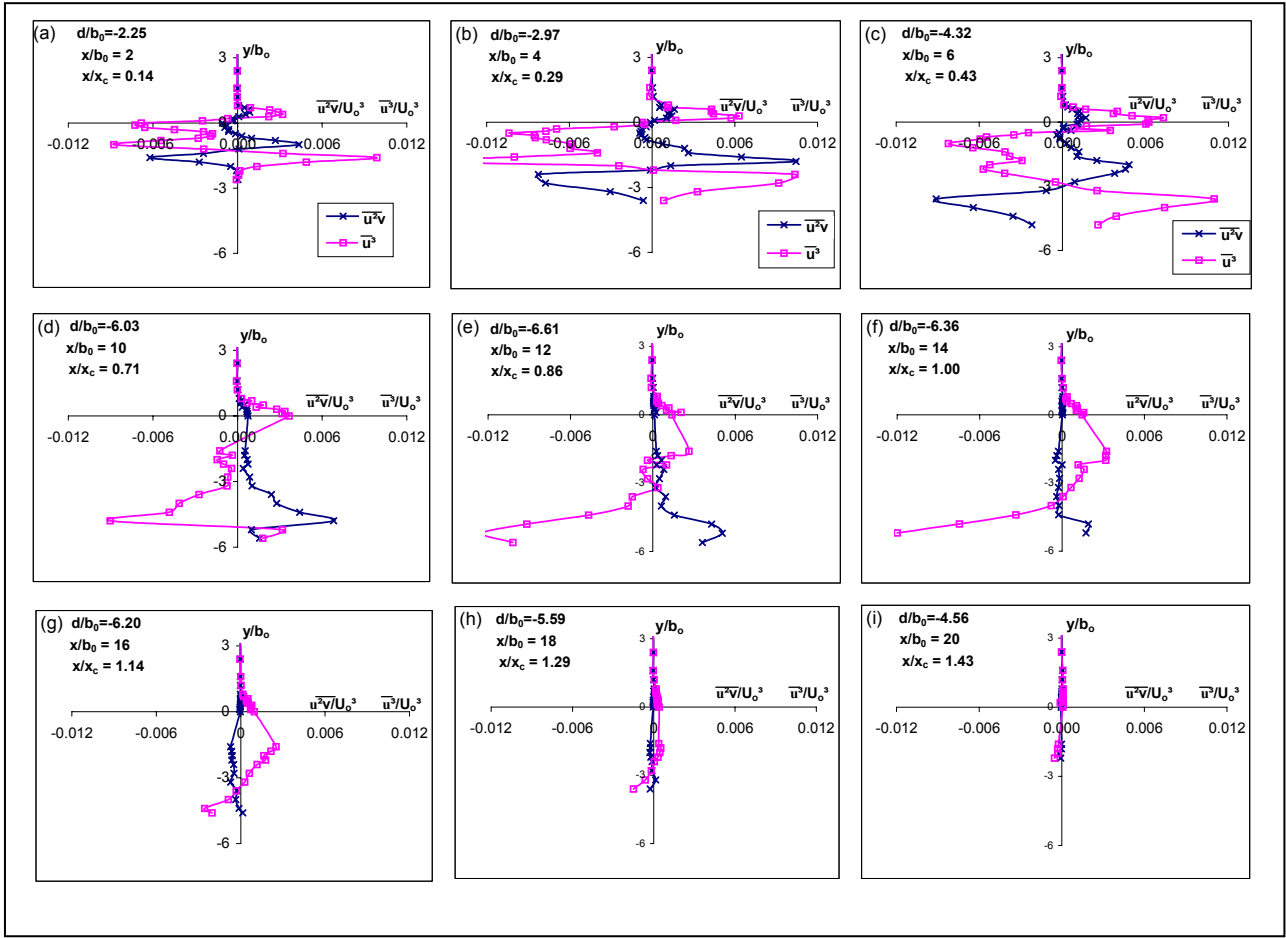


Figure 6: Variation of $\overline{u^2v}$ and $\overline{u^3}$ at various axial stations (Test A).

whereas $\overline{u^3}$ has a positive peak. The peak value of $\overline{u^3}$ is larger than that of D_v . This indicates strong sweeping type motion in the flow direction that is partly directed towards the bed. If one were to extrapolate this flow process to earlier time periods, such sweeping motions could influence scour significantly. For locations farther up ($y/b_0 \geq -1.6$), absolute values of both D_v and $\overline{u^3}$ decrease and become zero at almost the same level ($y/b_0 = -1.2$). This has significance as the changeover of sign indicates change in type of motion (ejection vs. sweep). Beyond this point, again absolute values of both D_v and $\overline{u^3}$ increase and attain local peak values at $y/b_0 = -1.0$, but once again with opposite sign. This time, D_v has a positive peak whereas $\overline{u^3}$ has a negative peak. Similar to the earlier peak values, the peak value of $\overline{u^3}$ is larger than peak value of D_v . This indicates an upward transport of u momentum, where as $\overline{u^3}$ is negative, indicating a slower moving fluid parcel. With further increasing y/b_0 , both the variables approach zero. At $y/b_0 = -0.4$ (which is also the location of maximum \overline{U}), $\overline{u^2v}$ attains a zero value. Further increase in y/b_0 (≈ -0.1) indicates that both variables attain local peak values and both are negative. This indicates fluid particles enter the jet as entrainment from above the jet centerline. Just above the nozzle

centerline ($y/b_0 = 0.4$), $\overline{u^2v}$ and $\overline{u^3}$ both are positive, albeit slightly. This indicates that the fluid particle is being ejected and simultaneously moving a bit faster in the flow direction. Above this point, the value of both the variables reduces to almost zero and remains so for the rest of the depth. These have no direct influence on the effect of turbulence on scour.

Figure 6b shows characteristics, which are similar to that shown in Figure 6a. However, the magnitudes of the peaks are larger, which is indicative of larger level of turbulence activity. Figure 6c shows characteristics, which are similar to that shown in Figures 6a and 6b. Figure 6d shows both positive peak values (albeit very low) for $\overline{u^2v}$ and $\overline{u^3}$ near the bed ($y/b_0 = -5.6$). This is an indication of tendency for the fluid parcels to move in an upward direction. At this station, for $y/b_0 = -4.8$, both D_v and $\overline{u^3}$ attain peak values. D_v attains a positive peak whereas $\overline{u^3}$ attains a negative peak. Similar to the earlier peak values, the peak value of $\overline{u^3}$ is larger than peak value of D_v . This indicates an upward transport of u momentum, where as $\overline{u^3}$ is negative indicates a slower fluid parcel motion. Together, $\overline{u^2v}$ and $\overline{u^3}$ indicate ejection of low speed fluid parcels that would be entrained into the jet. This type of motion can potentially

contribute to suspending individual grains that can be transported by the mean flow. Farther from the bed and towards the free surface, the absolute value of both $\overline{u^2v}$ and $\overline{u^3}$ reduces and have no direct influence on the effect of turbulence on scour. Figures 6e and 6f shows characteristics similar to that shown in Figure 6d and are all in the region of near-zero bed slope. Comparing Figure 6d with Figure 6e and 6f, one can note that the magnitude of peak for $\overline{u^3}$ increases and the magnitude of peak for $\overline{u^2v}$ decreases with increasing distance from nozzle and the jet-like characteristics diminish starting at Figure 6f and beyond. As one is close to the mean attachment point of the jet on the bed, the impingement causes large scale motion in all directions. This is reflected in the reduction of $\overline{u^2v}$ and $\overline{u^3}$ values. Figures 6h and 6i show the profiles in the positive slope region and indicate that the values for $\overline{u^2v}$ are close to zero throughout the depth of flow. This indicates very low turbulent diffusion in the y direction. For this region, there is a reduction in the streamwise turbulent flux with increasing distance from nozzle and eventually reaches zero, indicating a reduction in turbulent activities.

The ejection and sweeping type activities described above confirm the visual observations noted earlier. At the location of two prominent fluid structures (at asymptotic conditions), there is very large negative $\overline{u^3}$ values with low turbulent diffusion. This may be one of the causes for particle movement at this location.

IV. CONCLUSIONS

An experimental study was carried out to further understand the role of fluid structures in causing scour by plane jets. The study indicates the presence of different types of flow structures during various time periods. Both visual observation and velocity measurements aided in deciphering the role of the fluid structures. Even for regions near the nozzle, the present jet did not demonstrate free jet like characteristics as indicated by the velocity measurements. This is to be expected due to bed confinement on one side and the large scale recirculation zone situated above the jet on the other side. The growth rate of the jet is larger towards the bed due to the excess turbulence created by the water-bed interaction. The following are the main conclusions that can be drawn from the study:

1. The entire test duration, from the start of flow to the attainment of asymptotic conditions, can be divided in to five time zones. A time scale, denoted by the ratio of the length of the scour hole at asymptotic conditions to the jet exit velocity is used to normalize the five regimes. Each of the time zones had certain dominant flow features. The first time zone was accompanied by intense digging due to the direct shear action of the jet. Two or three longitudinal streaks and very prominent concave depressions were observed in the second time zone. A scoop and throw type event was noticed in the third and fourth of the time zones, while turbulent bursts were active during asymptotic conditions.

2. At asymptotic conditions, besides the turbulent bursts, two prominent scour mechanisms were also observed occurring on either side of the flume axis. Bed particles appeared to be spiraled towards the side walls and the flume axis due to this motion. It should be remarked that the back and forth movement of the impingement point, the frequent but random turbulent bursts and the two prominent scour mechanisms, all occurred at one time or the other.

3. At the asymptotic state, scour profile in the hole region is nominally two-dimensional across the width of the flume. However, in the mound region, the lateral profile is not two-dimensional and has two distinct peaks. These peaks occur closer to the side walls leaving a trough in center portion of the mound.

4. Jet impingement point on the bed moves back and forth and the mean location of impingement is close to the maximum scour depth. Wide range of variation in instantaneous velocity from positive to negative values is a clear indication of back and forth movement of jet.

5. Most of the turbulence activity occurs at the end of negative slope and continues till the start of positive bed slope region. Analysis of the triple correlations indicates sweep type events in the region which can contribute to scour. Ejection type activity also occur which suspend the bed particles and can be carried away by mean flow. Though the velocity measurements were conducted at asymptotic conditions, one can extrapolate to other time periods and conclude than the sweep and ejection contribute significantly to the scour process.

REFERENCES

- [1] Annandale, G.W. (2004). Keynote address, Second International Conference on Scour and Erosion. Singapore.
- [2] Balachandar, R., Kells, J.A., and Thiessen, R.J. (2000). "The effect of tailwater depth on the dynamics of local scour." *Canadian Journal of Civil Engineering*, 27(1),138-150.
- [3] Bey, A (2005), "Two-dimensional scour hole problem". M. A. Sc., thesis, Department of Civil and Environmental Engineering, University of Windsor, Canada.
- [4] Faruque, M. A. A. (2004). "Transient local scour by submerged three dimensional wall jets: Effect of tailwater depth." M. A. Sc., thesis, University of Windsor, Canada
- [5] Hogg, A. J., Huppert, H. E. and Dade, W.B. (1997). "Erosion by planar turbulent wall jets." *Journal of Fluid Mechanics*, 338, 317-340.
- [6] Hopfinger, E.J., Kurniawan, A., Graf, W. H., and Lemmin, U. (2004) "Sediment erosionby Götler vortices: the scour problem." *Journal of Fluid Mechanics*, 520, 327-342.
- [7] Rajaratnam, N. and Berry, B. (1977). "Erosion by circular turbulent wall jets." *Journal of Hydraulic Research*, 15(3), p 277-289.